Journal of Medicinal Chemistry

ACS AuthorChoice

Article

pubs.acs.org/jmc

Terms of Use

UNC2025, a Potent and Orally Bioavailable MER/FLT3 Dual Inhibitor

Weihe Zhang,[†] Deborah DeRyckere,[∥] Debra Hunter,[§] Jing Liu,[†] Michael A. Stashko,[†] Katherine A. Minson,[∥] Christopher T. Cummings,[∥] Minjung Lee,[∥] Trevor G. Glaros,[⊥] Dianne L. Newton,[⊥] Susan Sather,[∥] Dehui Zhang,[†] Dmitri Kireev,[†] William P. Janzen,[†] H. Shelton Earp,[‡,§] Douglas K. Graham,[∥] Stephen V. Frye,*[,†,§] and Xiaodong Wang*[,†]

[†]Center for Integrative Chemical Biology and Drug Discovery, Division of Chemical Biology and Medicinal Chemistry, Eshelman School of Pharmacy, [‡]Department of Pharmacology, School of Medicine, and [§]Lineberger Comprehensive Cancer Center, Department of Medicine, School of Medicine, University of North Carolina at Chapel Hill, Chapel Hill, North Carolina 27599, United States

[∥]Department of Pediatrics, School of Medicine, University of Colorado Denver, Aurora, Colorado 80045, United States

[⊥]Biological Testing Branch, Developmental Therapeutics Program, Leidos Biomedical Research, Inc, Frederick National Laboratory for Cancer Research, Frederick, Maryland 21702, United States

Supporting Information

ABSTRACT: We previously reported a potent small molecule Mer tyrosine kinase inhibitor **UNC1062**. However, its poor PK properties prevented further assessment in vivo. We report here the sequential modification of **UNC1062** to address DMPK properties and yield a new potent and highly orally bioavailable Mer inhibitor, **11**, capable of inhibiting Mer phosphorylation in vivo, following oral dosing as demonstrated by pharmaco-dynamic (PD) studies examining phospho-Mer in leukemic blasts from mouse bone marrow. Kinome profiling versus more than 300 kinases in vitro and cellular selectivity assessments demonstrate that **11** has similar subnanomolar activity against Flt3, an additional important target in acute myelogenous leukemia (AML), with pharmacologically useful selectivity versus other kinases examined.

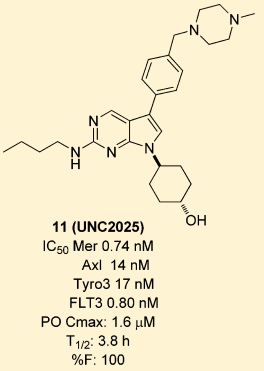

INTRODUCTION

Drug metabolism and pharmacokinetics (DMPK) are key elements to be optimized in drug development. Poor PK properties have historically been identified as one of the main contributors to failure in advancing new compounds toward approval as medicines, along with drug safety issues and lack of phase II efficacy. On the basis of a survey conducted by the U.S. Food and Drug Administration (FDA) in 1991, 39% of clinical failure resulted from unfavorable PK properties of clinical candidates, including poor bioavailability, high clearance, low solubility, and difficult formulation.[1] Since that time, medicinal chemists have focused on improvement of DMPK in the early drug discovery phase, allowing unsuitable compounds to be filtered out as these properties are optimized. This change was enabled by major improvements utilizing mass spectrometry of unlabeled compounds and has been further facilitated by the introduction of higher throughput in vitro and in vivo DMPK methodologies as well as in silico modeling techniques to help predict the effects that structural changes have on individual PK parameters.[2] Consequently, by the year 2000, the attrition rate of compounds due to poor DMPK dropped to less than 10%.[1] Although multiple reports of medicinal chemistry efforts to improve DMPK properties of selected compounds exist,[3] the process relies heavily on trial and error, and it remains challenging to optimize the DMPK profile for a given compound while retaining the required pharmacological profile. This manuscript presents our approach to improve the DMPK of an in vitro tool compound to generate an orally bioavailable lead targeting two receptor tyrosine kinases, Mer and the Fms-like tyrosine kinase 3 (Flt3).

Mer receptor tyrosine kinase (RTK) belongs to the Tyro3, Axl, and Mer (TAM) family of RTKs.[4] Abnormal expression and activation of Mer has been implicated in the oncogenesis of many human cancers,[5] including acute lymphoblastic leukemia (ALL),[6] acute myeloid leukemia (AML),[7] nonsmall cell lung cancer (NSCLC),[8] melanoma,[9] and glioblastoma,[10] where Mer functions to increase cancer cell survival, thereby promoting tumorigenesis and chemoresistance.[7−9,10a,11] Mer has recently been identified as a potential therapeutic target in leukemia and several types of solid tumors by demonstration that shRNA-mediated Mer inhibition abrogated oncogenic phenotypes, including decreased clonogenic growth, enhanced chemosensitivity, and delayed tumor progression in animal models. Similarly, activating mutations in Flt3, especially internal tandem duplications (ITD) in the juxtamembrane domain,

Received: May 14, 2014
Published: July 28, 2014

   dx.doi.org/10.1021/jm500749d | J. Med. Chem. 2014, 57, 7031−7041

are detected in approximately 30% of adult and 15% of childhood AMLs.[12] In AML, Flt3 ITD is considered to be a classic oncogenic driver.[12] Clinical responses to early Flt3 inhibitors were largely limited to transient reductions in peripheral blood and bone marrow blasts.[13] This has been attributed to insufficient Flt3 inhibitory activity and high toxicity of early compounds due to broad spectrum kinase inhibition.[14] Subsequently, enhanced potency Flt3 inhibitors with more selective kinase inhibitory profiles have been advanced and have demonstrated significant clinical activity, though none have been approved to date for the treatment of AML.[14] Since the Mer RTK is aberrantly expressed in ALL, and widely expressed in non-Flt3 mutant AML, an inhibitor demonstrating potent activity against both Mer and Flt3 with selectivity versus other kinases could be widely applicable in leukemias. A compound with this profile would additionally provide a chemical tool to assess the degree to which combined antisurvival and antichemoresistance activity, due to Mer inhibition, can augment inhibition of an oncogenic driver such as the Flt3-ITD mutation.

RESULTS AND DISCUSSION

Pyrrolo[2,3-*d*]pyrimidine Scaffold Improves DMPK. To date, there are only a few kinase-targeted compounds that have been designed intentionally as Mer inhibitors,[15] such as **UNC1062** (**1**),[15b] while others were developed for different purposes but have Mer inhibitory activity as part of their kinase profiles.[16] Consequently, none of the latter reported inhibitors are believed to demonstrate pharmacology primarily related to Mer inhibition. We previously showed that compound **1** is a potent Mer inhibitor (IC_{50} 1.1 nM) that blocked Mer phosphorylation in cell-based assays, including 697 B-ALL, BT-12 pediatric rhabdoid tumor, NSCLC, and melanoma cell lines.[13b] This compound also decreased colony formation in solid tumor cell lines.[9a,15b] Surprisingly, kinome profiling revealed that **1** was also very potent against Flt3 (IC_{50} 3.0 nM) despite the relatively low overall homology between Mer and Flt3 kinase domains (42% identity) and significant differences within their ATP binding sites. While Flt3 activity lessens the utility of this lead as a specific chemical probe for Mer kinase,[17] the potential therapeutic utility of a dual inhibitor is compelling and warranted further development. Separate optimization efforts are being focused on development of even more selective Mer specific compounds. In addition, because of low solubility and absence of oral exposure, compound **1** was subjected to further chemical improvement to render it suitable for in vivo study. Therefore, the solubility and PK properties of **1** were addressed, while its activity and kinome profile were maintained in order to advance a Mer/Flt3 inhibitor as an agent to treat AML and ALL.

On the basis of the reported X-ray structure of the **UNC569**/Mer complex,[15a] the N2 nitrogen on the pyrazole ring appears to make no specific interactions with the Mer protein and therefore replacement with a carbon to introduce a new core structure, a pyrrolopyrimidine, was investigated. As shown in Scheme 1, the corresponding analogue of **1** in the pyrrolopyrimdine scaffold is **2** and we subsequently discovered that this modification resulted in improved solubility for members of this series during formulation for DMPK studies.

Synthesis of Pyrrolo[2,3-*d*]pyrimidines. Although there is only one difference (N vs CH) between compounds **1** and **2**, the synthesis of **2** is distinct (Scheme 2). While the reaction sequence could be varied during the synthesis of pyrazolopyrimidines to enable late-stage variation at each substituent position,[15a,18] the *trans*-4-hydroxycyclohexyl group was most efficiently attached to the nitrogen at the N1 position of the pyrrole ring early in the synthesis of pyrrolopyrimidines. In addition, the *N*-alkylation reaction to introduce a *trans*-4-hydroxycyclohexyl group at the N1 position of **1** did not work for **2**. Instead, a Mitsunobu reaction was used to introduce this substituent. As shown in Scheme 2, commercially available 5-bromo-2-chloro-7*H*-pyrrolo[2,3-*d*]pyrimidine (**3**) was chosen as the starting material and was converted to intermediate **5** by treatment with mono-TBS protected *cis*-cyclohexane-1,4-diol **4** in the presence of freshly prepared cyanomethylenetrimethyl phosphorane (CMMP) in 72% yield.[18] The S_NAr replacement of the chloride in **5** with butylamine under microwave irradiation at 150 °C yielded compound **6**. Suzuki-Miyaura coupling reaction of **6** with boronic acid **7** led to compound **8**. Finally, compound **2** was obtained in good yield (36% over 3 steps) following removal of the TBS group from **8** by treatment with 1% HCl.

Scheme 1. Pyrrolopyrimidine Analogue 2

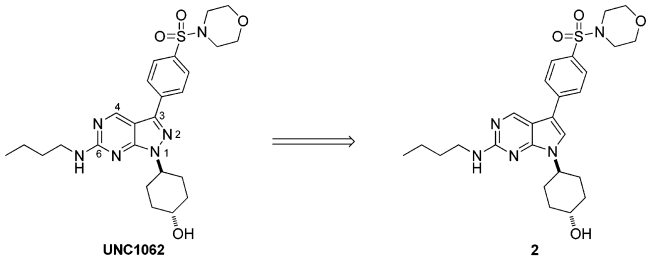

PK Property Improvement of Pyrrolo[2,3-*d*]-pyrimidines. It was determined that compound **2** had similar activity and selectivity profiles (IC_{50}'s: Mer, 0.93 nM; Axl, 29 nM; Tyro3, 37 nM; Flt3, 0.69 nM) as **1** within the TAM family. In addition, **2** had a lower melting point (215.4−216.2 °C) than **1** (234.2−234.6 °C), which suggested it would have better solubility.[19] Indeed, **2** proved more soluble in DMPK formulations, and following intravenous (iv) or oral (po) administration in mice, **2** had better oral exposure as compared to **1** (Table 1). Mice were chosen for PK studies because they are an appropriate species for determination of therapeutic effects in preclinical leukemia models. Taken together, these data indicated that this scaffold modification approach to improving the PK properties of **1** was promising. However, the structure of **2** needed to be fine-tuned to further address PK limitations such as high clearance.

In order to decrease the metabolic clearance of **2**, we considered modifications at each substituent position to either decrease log *P*, increase solubility, or decrease cytochrome P450 oxidation while retaining Mer/Flt3 potency. Our hypothesis that P450 oxidation was the dominant route of clearance was based on prior experience with compounds of this log *P* and molecular weight.[20] Re-examination of the SAR of the pyrazolopyrimidine scaffold revealed that a *trans*-4-hydroxycyclohexyl group at the N1 position was optimal, while alternative substitutions at this position either compromised the Mer potency or introduced undesired hERG activity.[15a,b] Therefore, this substituent was fixed. However, SAR in the pyrazolopyrimidines demonstrated that the butylamine group at the C6 position could be replaced with other aliphatic groups

dx.doi.org/10.1021/jm500749d | J. Med. Chem. 2014, 57, 7031−7041

Scheme 2. Synthesis of 2

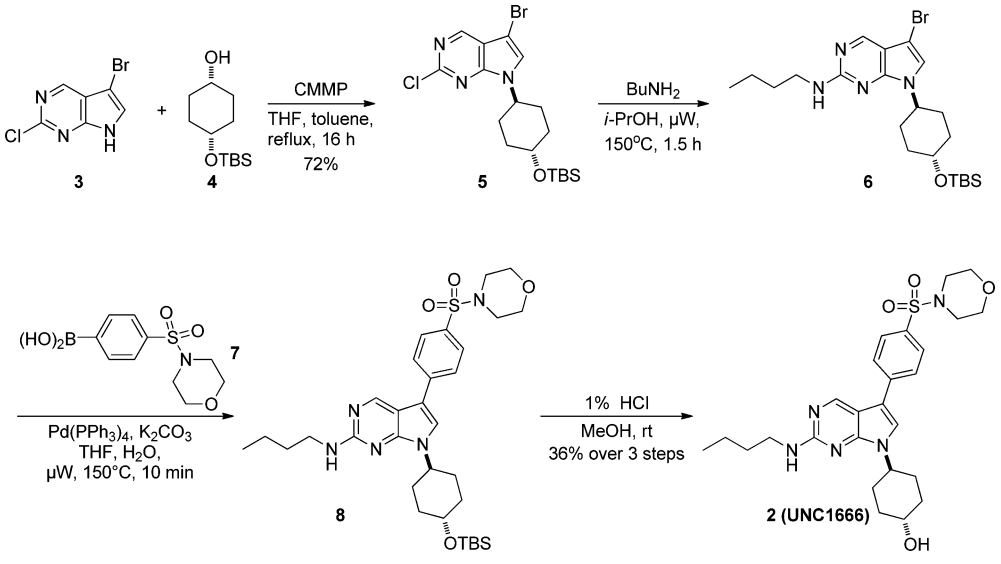

Table 1. In Vivo PK Parameters of 1 and 2 (n = 3 Mice Per Time Point)

	iv[a]					po[b]			
compound	$T_{1/2}$ (h)	C_{max} (μM)	AUClast (h μM)	Vss (L/kg)	CL (mL/min/kg)	T_{max} (h)	C_{max} (μM)	AUClast (h μM)	%F
1[c]	2.3	16	3.3	0.43	30	0.5	0.013	0.01	0.3
2[d]	0.23	7.9	1.4	0.78	70	0.25	0.16	0.12	8.4

[a]iv Dose at 3 mg/kg. [b]po Dose at 3 mg/kg. [c]iv Formulation: 7.5% v/v *N*-methyl pyrrolidone; 20% cremophor EL in water. [d]iv Formulation: 5% NMP, 5% solutol HS in normal saline.

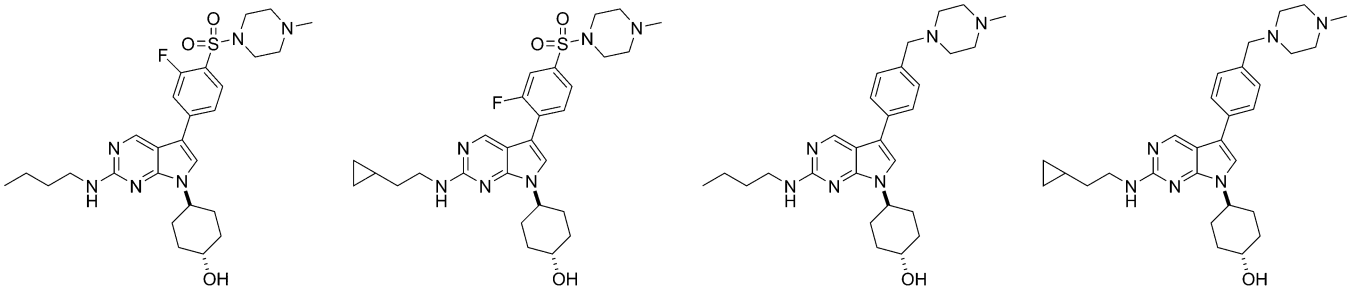

Figure 1. Structures and enzymatic activity of **9**–**12**.

Table 2. In Vivo Pharmacokinetic Parameters of 9–12 (n = 3 Mice Per Time Point)

	iv						po				
compound	dose (mg/kg)	$T_{1/2}$ (h)	C_{max} (μM)	AUClast (h μM)	Vss (L/kg)	CL (mL/min/kg)	dose (mg/kg)	T_{max} (h)	C_{max} (μM)	AUClast (h μM)	% F
9[a]	1	0.80	0.40	0.27	5.5	103	10	0.25	0.39	0.66	25
10[b]	3	1.2	1.2	1.0	5.3	76	3	0.25	0.42	0.69	67
11[c]	3	3.8	4.1	9.2	2.3	9.2	3	0.50	1.6	9.2	100
12[c]	3	4.4	6.5	12	2.0	7.2	3	1.0	1.3	9.0	78

[a]iv Formulation: 7.5% v/v *N*-methyl pyrrolidone; 40% v/v PEG-400 in normal saline. [b]iv Formulation: 5% DMSO, 5% solutol in normal saline. [c]iv Formulation: normal saline (0.9% NaCl).

and Mer potency retained. Additionally, substituents at the C3 position were positioned toward the solvent front in X-ray cocrystal structures, and we reasoned that different solubilizing groups might be well-tolerated at this position.[15b] We therefore proceeded to make simultaneous changes in the C3 and C6 positions in order to rapidly explore their combined effect on

dx.doi.org/10.1021/jm500749d | J. Med. Chem. 2014, 57, 7031–7041

Scheme 3. Scale-up Route for 11

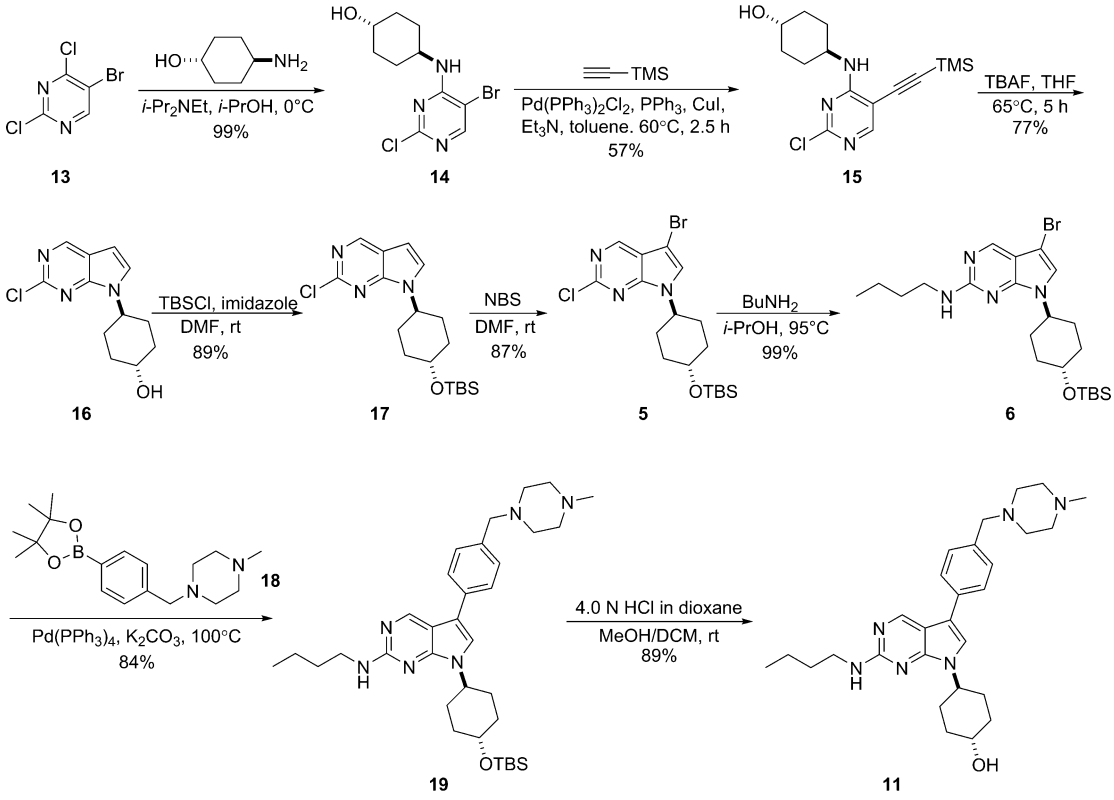

DMPK properties in an economically feasible fashion. This modification strategy led to analogues **9**–**12** (Figure 1), which were synthesized using the synthetic route presented in Scheme 2.

Similar to **2**, these analogues were potent against both Mer and Flt3 and had some selectivity over Axl and Tyro3. Compound **9** incorporated a basic, solubilizing *N*-methyl piperazine group on the phenyl ring in addition to a 3-fluoro substituent. As shown in Table 2, this led to increased oral bioavailability (25%, 3 fold better than **2**), although the clearance of **9** was still high (103 mL/min/kg) (Table 2). To further improve the metabolic stability of **9**, we tried to identify and block potential metabolic hot spots in the molecule. Two positions were explored simultaneously: fluorination of the meta position of the sulfonamide group on the phenyl ring and replacement of the butyl side chain of **9** by cyclopropyl ethyl to create analogue **10**.[21] On the basis of published studies with simple alkanes, the C–H bond strength of the cyclopropyl ring exceeds that of the terminal $-CH_3$ of the butyl group in **9** by approximately 7 kcal/mol, suggesting that this substituent might result in diminished P450-mediated oxidation liability for this aliphatic chain.[22] Indeed, analogue **10** demonstrated reduced clearance (76 mL/min/kg) and better oral bioavailability (67% vs 25% for **9**). We hypothesized that removing the sulfonamide group of **9** might be another way to further increase its solubility and improve PK properties, as sulfonamides are known to have high melting points relative to the corresponding amines.[23] As a result, analogue **11** (**UNC2025**) was prepared and demonstrated excellent PK properties: low clearance (9.2 mL/min kg), longer half-life (3.8 h), and high oral exposure (100%) (Table 2). Furthermore, the HCl salt of **11** was highly soluble in normal saline (kinetic solubility: 38 μg/mL, pH = 7.4). Substitution of **11** with a cyclopropyl ethyl side-chain resulted in **12**, which demonstrated a further modest decrease in clearance, consistent with some contribution of P450 metabolism of the C3 side-chain to metabolic stability but with very similar overall PK properties to **11**. With excellent solubility and PK properties, as well as a much less expensive C3 substituent versus **12**, analogue **11** was chosen for further studies, including kinome selectivity profiling, cell-based assays, and pharmacodynamic assays using a mouse model to determine the activity of the compound in leukemic blasts in vivo.

Scale-up Route for 11. In vivo studies require gram quantities of compound, and although the synthetic route presented in Scheme 2 was successfully applied to prepare analogs for SAR purposes, it was costly and difficult to perform on a multigram scale, especially the Mitsunobu reaction. Large-scale preparation of the CMMP required for this reaction was also challenging. Therefore, an alternative synthetic route for the large-scale synthesis of **11** was developed, as shown in Scheme 3. Starting with readily available 5-bromo-2,4-dichloropyrimidine (**13**), compound **14** was obtained in quantitative yield after an S_NAr replacement of the 4-chloro group with *trans*-4-aminocyclohexanol. A Sonogashira coupling reaction between **14** and ethynyltrimethylsilane yielded intermediate **15**, which was converted to intermediate **16** by in situ deprotection of the TMS group and formation of the pyrrole ring in 77% yield. To ease purification in the next few steps, the hydroxyl group of **16** was protected with a TBS protecting group to yield **17**. Bromination of **17** with NBS provided compound **5** which was converted to **6** via a second S_NAr replacement reaction with butylamine in high yield. Finally, analogue **11** was obtained by a Suzuki-Miyaura cross coupling reaction of **6** with 4-(4-methylpiperazino)-methylphenylboronic acid pinacol ester **18** in the presence of

dx.doi.org/10.1021/jm500749d | J. Med. Chem. 2014, 57, 7031–7041

Table 3. Carna IC_{50} of the Top 10 kinases and Met kinase Inhibited by 11

Kinase	FLT3	MER	AXL	TRKA	TRKC	QIK	TYRO3	SLK	NuaK1	KIT	Met
IC_{50} (nM)	0.35	0.46	1.65	1.67	4.38	5.75	5.83	6.14	7.97	8.18	364
sequence identity	0.42	1.0	0.70	0.37	0.34	0.24	0.65	0.36	0.25	0.41	0.48

$Pd(PPh_3)_4$ and K_2CO_3 followed by deprotection of the TBS group. Although this reaction sequence is longer compared to the one shown in Scheme 2, each reaction in this sequence can be easily scaled up and the overall yield is comparable (25% vs 26%). More than 170 g of **11** have been prepared via this route.

Selectivity Profiling. As most kinase inhibitors are ATP competitive and bind at a functionally conserved site, an understanding of selectivity within the context of the kinome is important for clinical development for two different but important reasons: (1) it is critical to understand which kinases are inhibited by in vivo concentrations of a drug candidate and contribute to the observed pharmacology in order to target the appropriate patients based on kinase mutational status and preclinical target validation based on shRNA and other gene-based approaches. (2) Multikinase inhibitors have demonstrated significant toxicity, and even though definition of individual kinase "anti-targets" is not well-developed, broad spectrum inhibitors are generally undesirable. Of these two issues, we focused on addressing the kinase pharmacology attributable to **11** most thoroughly at this stage. As there are numerous methods available for kinome profiling,[24] in vitro and in cells, we sought to obtain a data set for correlation across in vitro and cellular assays in order to best predict the pharmacology that would emerge from the kinome profile of **11**.

Therefore, the overall kinome profile of **11** was assessed in duplicate versus 305 kinases at Carna Biosciences using a microcapillary electrophoresis assay similar to our in house assay. A concentration of 100 nM was used as it is more than 100-fold above the IC_{50} determined in our in vitro assay for Mer kinase and would therefore capture other kinases that could be partially inhibited when Mer is inhibited by >90%. Sixty-six kinases were inhibited by more than 50% at this concentration.[25] IC_{50} values against these kinases were determined at their ATP Km, and the top 10 kinases inhibited by **11** are shown in Table 3. Gratifyingly, of the 305 kinases tested, **11** inhibited Mer and Flt3 with the greatest potency. Interestingly, the IC_{50} values against other kinases did not correlate with a sequence similarity to the Mer protein.[26] On the basis of protein sequence within the kinase domain, Met is the closest kinase to the TAM family, and many Met inhibitors also inhibit the TAMs.[26] However, **11** was more than 700-fold less active against Met compared to Mer, while it was equally potent against Flt3. In addition, the modest degree of selectivity of **11** for Mer over Axl and Tyro3 in this external profiling was roughly consistent with the selectivity estimated from our determination of their Morrison K_i's [Mer, 0.16 ± 0.06 nM (n = 9); Axl, 13.3 ± 8.3 nM (n = 4); Tyro3, 4.67 ± 2.82 nM (n = 5); Flt3, 0.59 ± 0.32 nM (n = 4)].[27] The in vitro observation that Mer and Flt3 were the kinases most potently inhibited by **11** was confirmed for Mer kinase in B-ALL 697 cell lysates using the ATP ActivX probe assay,[28] where it demonstrated an IC_{50} of 0.05 nM for Mer (although the redundancy of Mer and Tyro3 peptides does not distinguish these kinases). Despite the basic differences between these two assays, both indicated that Mer was a primary target for **11**. Reflecting on the selectivity considerations discussed above, we were curious to assess whether the potency of **11** versus the 8 other kinases in Table 3 (or kinases even less potently inhibited) could contribute significantly to its pharmacology. To begin to address this question, we decided to examine how well in vitro potency translated to inhibition of phospho-protein signaling in cells where the presence of serum protein, high intercellular concentrations of ATP, and cellular membrane permeability can significantly modulate compound activity.

Cellular Kinase Inhibition. In 697 B-ALL cells, **11** mediated potent inhibition of Mer phosphorylation with an IC_{50} of 2.7 nM (Figure 2). Similarly, in Flt3-ITD positive

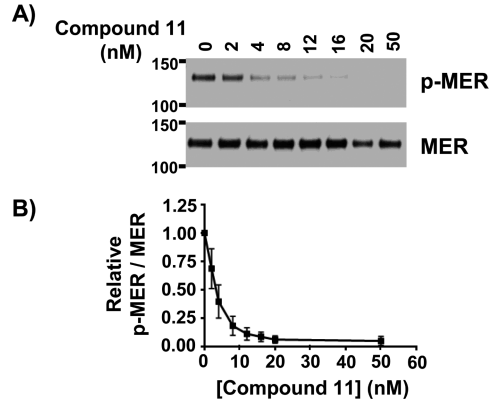

Figure 2. 11 Inhibits activation of Mer in acute leukemia cells. 697 Cells were treated with the indicated concentrations of **11** for 1 h. Pervanadate was added to cultures for 3 min to stabilize the phosphorylated form of Mer. Mer was immunoprecipitated from cell lysates, and total MER protein and Mer phosphoprotein (p-Mer) were detected by immunoblot. (A) Representative Western blots. (B) Relative levels of p-Mer and Mer proteins were determined by densitometry. Mean values ± standard error derived from 3 independent experiments are shown. IC_{50} = 2.7 nM with a 95% confidence interval from 1.8 to 4.2 nM.

Molm-14 acute myeloid leukemia cells, treatment with **11** resulted in decreased phosphorylation of Flt3 with an IC_{50} of 14 nM (Figure 3). This phospho-protein readout is predictive of biological consequences attributable to these kinases, as incubation with **11** resulted in significant inhibition of colony formation in soft agar cultures of the A549 NSCLC and Molm-14 AML cell lines, which are known to be dependent on Mer[8] and Flt3,[29] respectively, for optimal expression of oncogenic phenotypes (Figure 4). In contrast, a negative control compound **20**, a structurally similar but much weaker Mer and Flt3 inhibitor (Figure 4C), had no significant effect on colony-forming potential in either cell line. It is noteworthy that the correlation of biological effect as compared to phospho-protein inhibition IC_{50} correlates most closely for the ITD driver mutation in Flt3 (EC_{50} for colony formation inhibition = IC_{50} for p-Flt3 inhibition, Figure 4B), while the biological effect attributed to Mer inhibition is right-shifted as compared to phospho-protein inhibition (EC_{50} for colony formation inhibition > IC_{50} for p-Mer inhibition, Figure 4A). Since it is difficult to reject the hypothesis that this right-shift is due to the need to inhibit a kinase other than Mer in the NSCLC colony

dx.doi.org/10.1021/jm500749d | J. Med. Chem. 2014, 57, 7031−7041

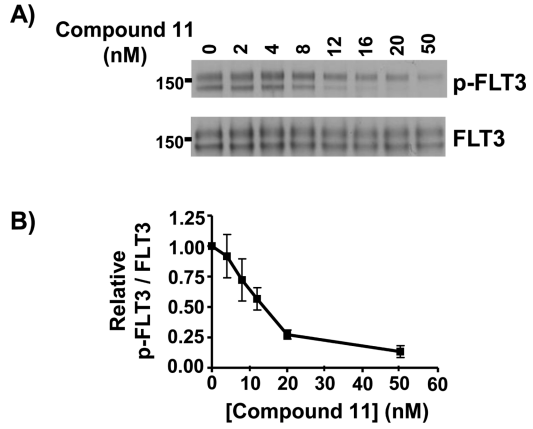

Figure 3. 11 Inhibits activation of Flt3 in acute leukemia cells. Flt3-ITD positive Molm-14 cells were treated with the indicated concentrations of **11** for 1 h. Pervanadate was added to cultures for 3 min to stabilize the phosphorylated form of Flt3. Flt3 was immunoprecipitated from cell lysates and total Flt3 protein and Flt3 phosphoprotein (p-Flt3) were detected by immunoblot. (A) Representative Western blots. (B) Relative levels of p-Flt3 and Flt3 proteins were determined by densitometry. Mean values ± standard error derived from 3 independent experiments are shown. IC_{50} = 14 nM with a 95% confidence interval from 8.4 to 24 nM.

formation assay, we decided to further explore the potency of **11** versus other kinases appearing in the selectivity data of Table 3.

Because of their high degree of similarity to Mer, our overall interest in the TAM family, and the significant inhibition by **11** in enzymatic assays, Axl and Tyro3 were chosen from Table 3 as sentinel kinases to further evaluate the selectivity of **11** in cell-based phospho-protein assays. In order to facilitate this comparison in a systematic fashion, chimeric proteins consisting of the extracellular and transmembrane domains from the epidermal growth factor receptor (EGFR) and the intracellular domain from Mer, Axl, or Tyro3 were expressed in 32D cells such that all three proteins could be identically stimulated with the EGF ligand for direct comparison. In this system, **11** mediated potent inhibition of the chimeric Mer protein with an IC_{50} of 2.7 nM (Figure 5), identical to its activity against endogenous Mer in 697 cells and consistent with the validity of this system for evaluation of selectivity. In contrast, much higher concentrations of **11** were required to effectively inhibit phosphorylation of Axl (IC_{50} = 122 nM) and Tyro3 (IC_{50} = 301 nM). Thus, the approximately 4- to 13-fold difference in activity for Mer relative to Axl and Tyro3 in Carna IC_{50} profiling (Table 3) translated to 40- to 100-fold selectivity for Mer over Axl and Tyro3, respectively, in phospho-protein readouts in cell-based assays. The simplest explanation for this difference in fold selectivity is that the Mer IC_{50} (0.46 nM) slightly underestimates the true potency of **11** as seen when the method of Morrison is used to determine its K_i, which is equal to 160 picomolar, while the Carna IC_{50}'s are more reflective of the potency of **11** versus Flt3, Axl, and Tyro3. In fact, a plot of in vitro potency versus cellular phospho-protein potency that utilizes the Mer K_i and the Carna IC_{50}'s for Flt3, Axl, and Tyro3 (Figure 6) results in a correlation coefficient (R^2) of 0.98 with a predicted 50-fold shift in potency in the cellular assay environment relative to Carna IC_{50}'s. With this correlation in mind, we proceeded to evaluate how effectively **11** could inhibit Mer phosphorylation in vivo in order to establish pharmacodynamic evidence of target engagement and assess the drug concentrations required and how they relate to potential engagement of other kinase targets.

Pharmacodynamic Evaluation. To determine whether **11** can mediate inhibition of target proteins in vivo, we generated mice with human leukemia xenografts. In these mice, a single 3 mg/kg dose of **11** administered orally was sufficient to decrease Mer phospho-protein levels in bone marrow leukemia cells by greater than 90% (Figure 7). The plasma concentration of **11** at the time of bone marrow collection can be estimated to be approximately 1.6 μM based on the PK data shown in Table 2. In order to relate this concentration to the IC_{50} versus p-Mer, we determined the plasma protein binding of **11** in mice to be 98.6% ± 0.4% (n = 3), resulting in a free fraction concentration of approximately 22 nM, 30 min after a 3 mg/kg oral dose. As this is roughly 10-fold above the cellular IC_{50} versus p-Mer (Figure 2), inhibition of p-Mer in vivo by >90% at a 3 mg/kg oral dose is consistent with expectations at a 30 min time point after dosing (see the Supporting Information for calculation of % I versus free fraction based on K_i and cellular potency for **11**).

These data for in vivo inhibition of p-Mer enable an estimate of the kinome pharmacology profile of **11** in vivo using the following assumptions: (1) in vitro potency translates to cellular phospho-protein potency for all kinases in the same way as for the TAMs and Flt3 (Figure 6); (2) pharmacological effects in vivo resulting from inhibition of a particular kinase require >90% inhibition of phospho-protein signaling from that kinase; (3) selectivity estimated at C_{max} is indicative of overall pharmacological selectivity. Figure 8 is a ranked plot of the

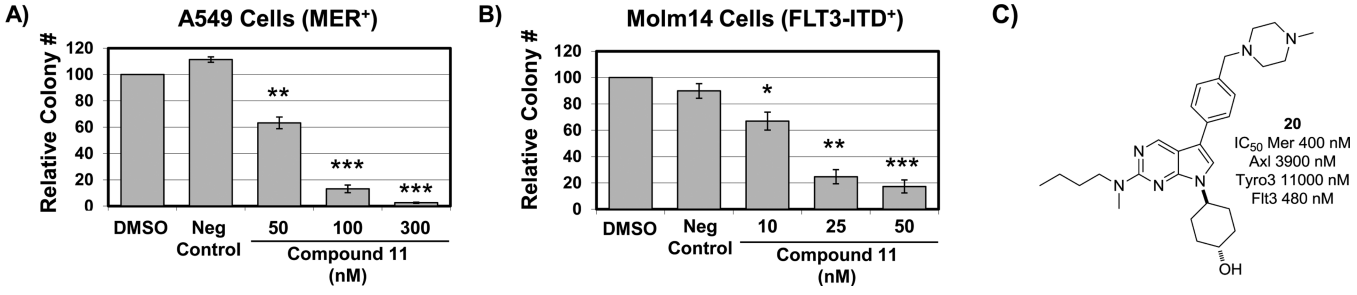

Figure 4. 11 Inhibits colony formation in Mer-dependent and Flt3-dependent tumor cell lines. (A) A549 NSCLC cells or (B) Molm-14 AML cells were cultured in 0.35% soft agar overlaid with medium containing **11**, a negative control (**20**) (300 nM for A549 NSCLC cells and 50 nM for Molm-14 AML cells), or vehicle. Medium and compounds were refreshed 3 times per week. Colonies were stained and counted. Mean values ± standard error derived from 3 to 4 independent experiments are shown. Statistically significant differences were determined using the student's paired t test (* $p < 0.05$, ** $p \leq 0.005$, ***$P < 0.0005$ relative to vehicle only). (C) Structure and enzymatic IC_{50}'s of compound **20**.

dx.doi.org/10.1021/jm500749d | J. Med. Chem. 2014, 57, 7031−7041

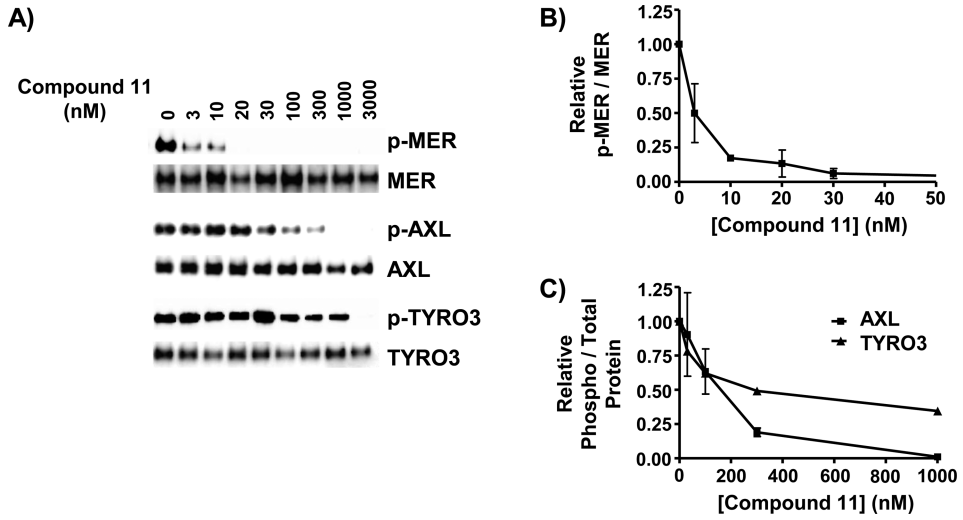

Figure 5. 11 Selectively inhibits Mer in cell-based assays. 32D Cells stably expressing chimeric receptors consisting of the extracellular ligand-binding and transmembrane domains of the EGF receptor and the intracellular kinase domain of Mer, Axl, or Tyro3 were treated with **11** or vehicle for 1 h prior to stimulation for 15 min with 100 ng/mL EGF. Chimeric proteins were immunoprecipitated from whole cell lysates and phospho-tyrosine-containing and total proteins were detected by Western blot. (A) Representative Western blots are shown. (B and C) Phosphorylated and total protein levels were determined by densitometry. Mean values ± standard error derived from 3 independent experiments are shown. IC_{50} values and 95% confidence intervals were determined by nonlinear regression and are 2.7 nM (1.7−4.2 nM) for Mer, 122 nM (64−230 nM) for Axl, and 301 nM (110−820 nM) for Tyro3.

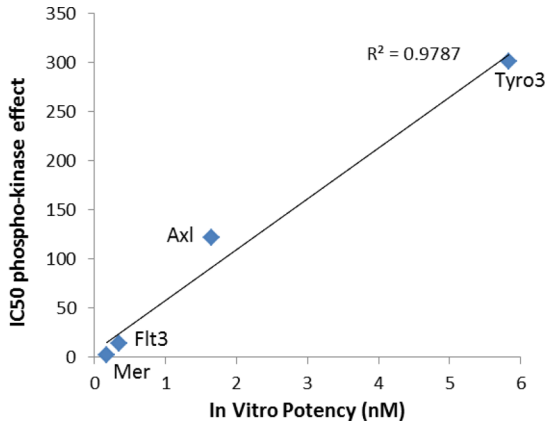

Figure 6. Correlation of in vitro and phospho-protein potency for **11** versus Mer, Flt3, Axl, and Tyro3 utilizing the Morrison K_i for Mer and the IC_{50}'s from Table 3 for all others.

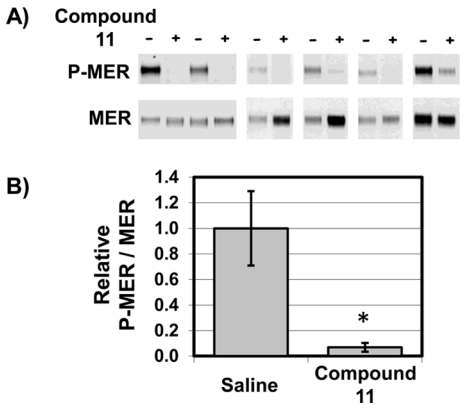

Figure 7. 11 Inhibits Mer phosphorylation in bone marrow leukemia cells in vivo. NOD/SCID/gamma mice were transplanted with 697 acute leukemia cells and allowed to engraft for 14 days. Leukemic mice were then treated with a single 3 mg/kg dose of **11** or saline vehicle administered by oral gavage. Femurs were collected 30 min later. Bone marrow cells were flushed and incubated for 10 min in the presence of 20% FBS and pervanadate phosphatase inhibitor to stabilize Mer phosphoprotein. Cell lysates were prepared and Mer was immunoprecipitated. (A) Phosphorylated and total Mer proteins were detected by Western blot. (B) Phosphorylated and total Mer protein levels were determined by densitometry. Mean values ± standard error are shown. Mer phosphoprotein was significantly decreased in leukemia cells collected from mice treated with **11** relative to mice treated with vehicle (0.07 ± 0.04 versus 1.00 ± 0.29; *(* p = 0.01, student's unpaired t test; n = 6).

kinases predicted to be most potently inhibited by **11** versus the free concentration required for 90% inhibition. This rank order differs from that of Table 3 due to the effect of varying ATP K_m's on the predicted inhibition of each kinase in vivo. For example, KIT has a particularly high K_m for ATP (370 μM) and is therefore predicted to be relatively easy to inhibit. At an oral dose of 3 mg/kg, **11** results in a C_{max} at 30 min of 22 nM (vertical line in Figure 8). Only Flt3 and Mer are inhibited by 90%, while TRKA, KIT, and Axl kinases are predicted to be partially inhibited at this dose. Tyro3 and the other kinases are minimally inhibited and would require free concentrations at least 10-fold higher for >90% inhibition to occur. Therefore, the pharmacology of **11** is most likely to be dominated by effects on Mer and Flt3, while Axl pharmacology can serve as an indicator of potential activity emerging from partial inhibition of other kinases such as KIT and TRKA. With the use of the data from a recent study of the selectivity of nine clinically approved RTK inhibitors for comparison,[25] **11** falls in the midground of selectivity profiles, being more selective than dasatinib, less selective than imatinib, and similar to pazopanib in terms of the number of other kinases inhibited when the most potently inhibited kinases are >90% inhibited (see Supporting Information for comparisons). Additionally, the unique rank order of kinases inhibited by **11** provides the basis for differentiation compared to these other RTK inhibitors, both for effectiveness when targeting Mer and Flt3 and perhaps

dx.doi.org/10.1021/jm500749d | J. Med. Chem. 2014, 57, 7031−7041

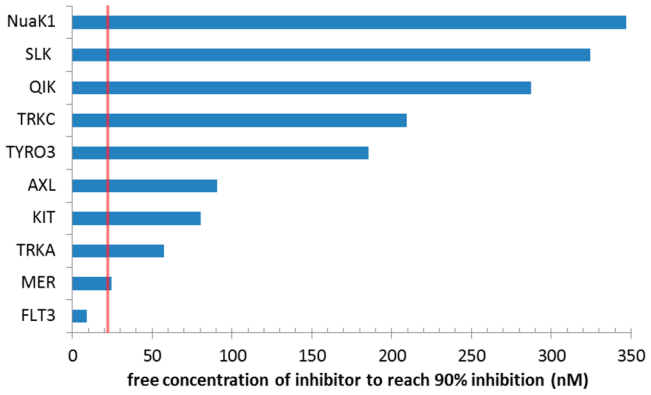

Figure 8. Predicted free concentration of **11** required in vivo for 90% inhibition of the top 10 kinases from Table 3. The vertical line corresponds to the measured free concentration of **11** at 30 min following a 3 mg/kg oral dose (Cmax, Table 2). (See the Supporting Information for methods and comparison to clinically approved RTK profiles assessed in the same manner.)

the side effect profile. While further efficacy studies and DMPK assessments in treated mice will be needed to fully validate the kinome basis for the preclinical pharmacology of **11**, this analysis provides a transparent and quantitative basis for study design and hypothesis testing.

In conclusion, we have successfully generated a potent, pharmacologically selective, and orally bioavailable Mer/Flt3 dual inhibitor **11** with improved solubility and DMPK properties relative to a previous in vitro tool compound **2**. Importantly, oral treatment with **11** resulted in effective target inhibition in bone marrow leukemia cells in an animal model. A cost-effective synthetic route for preparation of **11** was also developed to support in vivo preclinical studies.

EXPERIMENTAL SECTION

Details on the synthesis of all compounds are given in the Supporting Information. The purity of all tested compounds was determined by LC−MS and NMR to be >95%.

Kinome Profiling Using ActivX ATP/ADP Probes. Cellular lysate, inhibitor treatment, labeling reactions, digestion, and peptide capture were performed according to manufacturer's published protocols with modifications detailed below. Briefly, 697 B-ALL cells were gently pelleted, washed twice with PBS, lysed using MPER supplemented with HALT protease/phosphatase inhibitor cocktail (Pierce), and subjected to Zeba (Pierce) gel filtration spin columns to remove residual ATP and ADP. Following filtration, the final protein concentration was adjusted to 5.0 mg/mL using reaction buffer and supplemented with additional 1X HALT protease and phosphatase inhibitor cocktail. Lysate was aliquoted, snap frozen in liquid nitrogen, and stored at −80 °C until labeling. Prior to labeling, 2.5 mg of total lysate (final volume, 500 μL) was thawed to room temperature and treated with 10 μL of 1 M $MnCl_2$ for 1 min. Then the lysate was treated with or without **11** [0, 0.01, 0.1, 1.0, 10, 100, and 1000 nM] for 10 min. Following treatment, the ATP probe was added for 10 min at a final concentration of 5 μM. The labeling reaction was quenched with 500 μL of 10 M urea in MPER, 10 μL of 500 mM DTT, and heated to 65 °C for 30 min with shaking. Samples were cooled to room temperature and alkylated with 40 μL of a 1 M iodoacetamide solution for 30 min protected from light. The solution was then subjected to Zeba (Pierce) gel filtration and digested with 20 μg of trypsin at 37 °C for 2 h with shaking. 50 μL of a 50% high capacity streptavidin agarose slurry was added and allowed to incubate for 1 h at room temperature with constant mixing on a rotator. Agarose beads were then captured, washed, and eluted. Purified peptides were frozen, lyophilized, and stored at −80 °C. Immediately before mass spectrometric analysis, peptides were resuspended in 25 μL of 0.1% TFA. Details on mass spectrometry analysis and data analysis are provided in the Supporting Information.

Cell-Based Assays for Kinase Inhibition. 697 B-ALL cells and Molm-14 AML cells were cultured in the presence of **11** or vehicle-only for 1.0 h. Pervanadate solution was prepared fresh by combining 20 mM sodium orthovanadate in 0.9× PBS in a 1:1 ratio with 0.3% (w/w) hydrogen peroxide in PBS for 15−20 min at room temperature. Cultures were treated with 120 μM pervanadate for 3 min prior to collection, and cell lysates were prepared in 50 mM HEPES (pH 7.5), 150 mM NaCl, 10 mM EDTA, 10% glycerol, and 1% Triton X-100, supplemented with protease inhibitors (Roche Molecular Biochemicals, no. 11836153001). Mer and Flt3 proteins were immunoprecipitated with anti-Mer (R&D Systems, no. MAB8912) or anti-Flt3 (Santa Cruz Biotechnology no. sc-480) antibody and Protein G agarose beads (InVitrogen). Phospho-proteins were detected by Western blot using an antiphospho-Mer antibody raised against a peptide derived from the triphosphorylated activation loop of Mer[8] (Phopshosolutions, Inc.) or an antibody specific for phosphorylated Flt3 (Cell Signaling Technology, no. 3461). Nitrocellulose membranes were stripped and total proteins were detected using a second anti-Mer antibody (Epitomics Inc., no. 1633-1) or anti-Flt3 antibody (Santa Cruz Biotechnology no. sc-480). Relative phosphorylated and total protein levels were determined by densitometry using ImageJ, and IC_{50} values were calculated by nonlinear regression.

32D Cells expressing a chimeric EGFR-Mer, EGFR-Axl, or EGFR-Tyro3 receptor were cultured in the presence of **11** or vehicle-only for 1.0 h before stimulation with 100 ng/mL EGF (BD Biosciences no. 354010) for 15 min. Cells were centrifuged at 1000*g* for 5 min and washed with 1× PBS. Cell lysates were prepared in 20 mM HEPES (pH 7.5), 50 mM NaF, 500 mM NaCl, 5.0 mM EDTA, 10% glycerol, and 1% Triton X-100, supplemented with protease inhibitors (10 μg/mL leupeptin, 10 μg/mL phenylmethylsulfonyl fluoride, and 20 μg/mL aprotinin) and phosphatase inhibitors (50 mM NaF and 1.0 mM sodium orthovanadate). Mer protein was immunoprecipitated using a custom polyclonal rabbit antisera raised against a peptide derived from the C-terminal catalytic domain of Mer and Protein A agarose beads (Santa Cruz Biotechnology). Axl and Tyro3 proteins were immunoprecipitated using an antibody directed against a FLAG epitope engineered into the chimeric proteins (Sigma-Aldrich, no. F1804). Phosphotyrosine-containing proteins were detected by Western blot with a monoclonal HRP-conjugated antiphosphotyrosine antibody (Santa Cruz Biotechnology, no. sc-508). Antibodies were stripped from membranes, and total proteins were detected with the same antibodies used for immunoprecipitation.

Soft Agar Colony Formation Assays. A549 or Molm-14 cells were cultured in 1.5 mL of 0.35% soft agar containing 1× RPMI medium and 10% FBS and overlaid with 2.0 mL of 1× RPMI medium containing 10% FBS and the indicated concentrations of **11** or DMSO vehicle only. Medium and **11** or vehicle were refreshed 3 times per week. Colonies were stained with nitrotetrazolium blue chloride (Sigma-Aldrich, no. N6876) and counted after 2 weeks.

Pharmacodynamic Studies. NOD.Cg-*Prkdc*^{scid} *Il2rg*^{tm1Wjl}/SzJ (NSG) mice were transplanted with 2 × 10^6 697 B-ALL cells by intravenous injection into the tail vein, and leukemia was established for 14 days prior to treatment with a single dose of 3 mg/kg **11** or an equivalent volume (10 mL/kg) of saline vehicle. Pervanadate solution was prepared fresh, as described above. Femurs were collected from mice 30 min after treatment, and bone marrow cells were flushed with 1 mL of room temperature RPMI medium + 20% FBS + 1 μM $MgCl_2$ + 100 untis/ml DNase + 240 μM pervanadate and incubated at room temperature in the dark for 10 min. Bone marrow cells were collected by centrifugation at 4 °C, lysates were prepared, Mer protein was immunoprecipitated, and total and phospho-Mer proteins were detected and quantitated by Western blot, as described above.

dx.doi.org/10.1021/jm500749d | J. Med. Chem. 2014, 57, 7031−7041

■ ASSOCIATED CONTENT

Supporting Information

Experimental details and characterization of all compounds and biological methods. This material is available free of charge via the Internet at http://pubs.acs.org.

■ AUTHOR INFORMATION

Corresponding Authors

*Tel: 919-843-5486. E-mail: svfrye@email.unc.edu.

*Tel: 919-843-8456. E-mail: xiaodonw@unc.edu.

Notes

The authors declare the following competing financial interest(s): D.K., W.P.J., H.S.E., D.K.G., S.V.F., and X.W. have stock in Meryx, Inc.

■ ACKNOWLEDGMENTS

We thank Dr. Nancy Cheng, Ms. Wendy M. Stewart, and Ms. Yingqiu Zhou for their help with MCE assays. This work was supported by the University Cancer Research Fund and Federal Funds from the National Cancer Institute, National Institute of Health, under Contract HHSN261200800001E. Additional support was provided by NIH 1R01CA137078 (D.G.) and the BCRF (H.S.E.). The content of this publication does not necessarily reflect the views or policies of the Department of Health and Human Services, nor does mention of trade names, commercial products, or organizations imply endorsement by the U.S. Government.

■ REFERENCES

(1) Kola, I.; Landis, J. Can the Pharmaceutical Industry Reduce Attrition Rates? *Nat. Rev. Drug Discovery* **2004**, *3* (8), 711−716.

(2) Palmer, A. M. New Horizons in Drug Metabolism, Pharmacokinetics and Drug Discovery. *Drug News Perspect.* **2003**, *16* (1), 57−62.

(3) (a) Norman, M. H.; Andrews, K. L.; Bo, Y. Y.; Booker, S. K.; Caenepeel, S.; Cee, V. J.; D'Angelo, N. D.; Freeman, D. J.; Herberich, B. J.; Hong, F.-T.; Jackson, C. L. M.; Jiang, J.; Lanman, B. A.; Liu, L.; McCarter, J. D.; Mullady, E. L.; Nishimura, N.; Pettus, L. H.; Reed, A. B.; Miguel, T. S.; Smith, A. L.; Stec, M. M.; Tadesse, S.; Tasker, A.; Aidasani, D.; Zhu, X.; Subramanian, R.; Tamayo, N. A.; Wang, L.; Whittington, D. A.; Wu, B.; Wu, T.; Wurz, R. P.; Yang, K.; Zalameda, L.; Zhang, N.; Hughes, P. E. Selective Class I Phosphoinositide 3-Kinase Inhibitors: Optimization of a Series of Pyridyltriazines Leading to the Identification of a Clinical Candidate, AMG 511. *J. Med. Chem.* **2012**, *55* (17), 7796−7816. (b) Barlind, J. G.; Bauer, U. A.; Birch, A. M.; Birtles, S.; Buckett, L. K.; Butlin, R. J.; Davies, R. D. M.; Eriksson, J. W.; Hammond, C. D.; Hovland, R.; Johannesson, P.; Johansson, M. J.; Kemmitt, P. D.; Lindmark, B. T.; Gutierrez, P. M.; Noeske, T. A.; Nordin, A.; O'Donnell, C. J.; Petersson, A. U.; Redzic, A.; Turnbull, A. V.; Vinblad, J. Design and Optimization of Pyrazinecarboxamide-Based Inhibitors of Diacylglycerol Acyltransferase 1 (DGAT1) Leading to a Clinical Candidate Dimethylpyrazinecarboxamide Phenylcyclohexyl-acetic Acid (AZD7687). *J. Med. Chem.* **2012**, *55* (23), 10610−10629. (c) Coteron, J. M.; Marco, M.; Esquivias, J.; Deng, X.; White, K. L.; White, J.; Koltun, M.; El Mazouni, F.; Kokkonda, S.; Katneni, K.; Bhamidipati, R.; Shackleford, D. M.; Angulo-Barturen, I.; Ferrer, S. B.; Belen Jimenez-Diaz, M.; Gamo, F.-J.; Goldsmith, E. J.; Charman, W. N.; Bathurst, I.; Floyd, D.; Matthews, D.; Burrows, J. N.; Rathod, P. K.; Charman, S. A.; Phillips, M. A. Structure-Guided Lead Optimization of Triazolopyrimidine-Ring Substituents Identifies Potent Plasmodium falciparum Dihydroorotate Dehydrogenase Inhibitors with Clinical Candidate Potential. *J. Med. Chem.* **2011**, *54* (15), 5540−5561. (d) Stepan, A. F.; Mascitti, V.; Beaumont, K.; Kalgutkar, A. S. Metabolism-Guided Drug Design. *MedChemComm* **2013**, *4* (4), 631−652. (e) St Jean, D. J., Jr.; Fotsch, C. Mitigating Heterocycle Metabolism in Drug Discovery. *J. Med. Chem.* **2012**, *55* (13), 6002−6020.

(4) Chen, J.; Carey, K.; Godowski, P. J. Identification of Gas6 as a Ligand for Mer, a Neural Cell Adhesion Molecule Related Receptor Tyrosine Kinase Implicated in Cellular Transformation. *Oncogene* **1997**, *14* (17), 2033−2039.

(5) (a) Linger, R. M. A.; Keating, A. K.; Earp, H. S.; Graham, D. K. TAM Receptor Tyrosine Kinases: Biologic Functions, Signaling, and Potential Therapeutic Targeting in Human Cancer. *Adv. Cancer Res.* **2008**, *100*, 35−83. (b) Verma, A.; Warner, S. L.; Vankayalapati, H.; Bearss, D. J.; Sharma, S. Targeting Axl and Mer Kinases in Cancer. *Mol. Cancer Ther.* **2011**, *10*, 1763−1773.

(6) Graham, D. K.; Salzberg, D. B.; Kurtzberg, J.; Sather, S.; Matsushima, G. K.; Keating, A. K.; Liang, X. Y.; Lovell, M. A.; Williams, S. A.; Dawson, T. L.; Schell, M. J.; Anwar, A. A.; Snodgrass, H. R.; Earp, H. S. Ectopic Expression of the Proto-Oncogene Mer in Pediatric T-Cell Acute Lymphoblastic Leukemia. *Clin. Cancer Res.* **2006**, *12* (9), 2662−2669.

(7) Lee-Sherick, A.; Eisenman, K.; Sather, S.; McGranahan, A.; Armistead, P.; McGary, C.; Hunsucker, S.; Schlegel, J.; Martinson, H.; Cannon, C.; Keating, A. K.; Earp, H. S.; Liang, X.; DeRyckere, D.; Graham, D. K. Aberrant Mer Receptor Tyrosine Kinase Expression Contributes to Leukemogenesis in Acute Myeloid Leukemia. *Oncogene* **2013**, *32*, 5359−5368.

(8) Linger, R. M.; Cohen, R. A.; Cummings, C. T.; Sather, S.; Migdall-Wilson, J.; Middleton, D. H.; Lu, X.; Baron, A. E.; Franklin, W. A.; Merrick, D. T.; Jedlicka, P.; Deryckere, D.; Heasley, L. E.; Graham, D. K. Mer or Axl Receptor Tyrosine Kinase Inhibition Promotes Apoptosis, Blocks Growth and Enhances Chemosensitivity of Human Non-Small Cell Lung Cancer. *Oncogene* **2013**, *32*, 3420−3431.

(9) (a) Schlegel, J.; Sambade, M. J.; Sather, S.; Moschos, S. J.; Tan, A. C.; Winges, A.; Deryckere, D.; Carson, C. C.; Trembath, D. G.; Tentler, J. J.; Eckhardt, S. G.; Kuan, P. F.; Hamilton, R. L.; Duncan, L. M.; Miller, C. R.; Nikolaishvili-Feinberg, N.; Midkiff, B. R.; Liu, J.; Zhang, W.; Yang, C.; Wang, X.; Frye, S. V.; Earp, H. S.; Shields, J. M.; Graham, D. K. MERTK Receptor Tyrosine Kinase Is a Therapeutic Target in Melanoma. *J. Clin. Invest.* **2013**, *123* (5), 2257−2267. (b) Tworkoski, K. A.; Platt, J. T.; Bacchiocchi, A.; Bosenberg, M.; Boggon, T. J.; Stern, D. F. MERTK Controls Melanoma Cell Migration and Survival and Differentially Regulates Cell Behavior Relative to AXL. *Pigm. Cell Melanoma Res.* **2013**, *26* (4), 527−541.

(10) (a) Wang, Y.; Moncayo, G.; Morin, P., Jr.; Xue, G.; Grzmil, M.; Lino, M. M.; Clement-Schatlo, V.; Frank, S.; Merlo, A.; Hemmings, B. A. Mer Receptor Tyrosine Kinase Promotes Invasion and Survival in Glioblastoma Multiforme. *Oncogene* **2013**, *32* (7), 872−882. (b) Rogers, A. E. J.; Le, J. P.; Sather, S.; Pernu, B. M.; Graham, D. K.; Pierce, A. M.; Keating, A. K. Mer Receptor Tyrosine Kinase Inhibition Impedes Glioblastoma Multiforme Migration and Alters Cellular Morphology. *Oncogene* **2012**, *31* (38), 4171−4181.

(11) (a) Keating, A. K.; Salzberg, D. B.; Sather, S.; Liang, X.; Nickoloff, S.; Anwar, A.; Deryckere, D.; Hill, K.; Joung, D.; Sawczyn, K. K.; Park, J.; Curran-Everett, D.; McGavran, L.; Meltesen, L.; Gore, L.; Johnson, G. L.; Graham, D. K. Lymphoblastic Leukemia/Lymphoma in Mice Overexpressing the Mer (MerTK) Receptor Tyrosine Kinase. *Oncogene* **2006**, *25* (45), 6092−6100. (b) Keating, A. K.; Kim, G. K.; Jones, A. E.; Donson, A. M.; Ware, K.; Mulcahy, J. M.; Salzberg, D. B.; Foreman, N. K.; Liang, X.; Thorburn, A.; Graham, D. K. Inhibition of Mer and Axl Receptor Tyrosine Kinases in Astrocytoma Cells Leads to Increased Apoptosis and Improved Chemosensitivity. *Mol. Cancer Ther.* **2010**, *9* (5), 1298−1307. (c) Brandao, L.; Winges, A.; Christoph, S.; Sather, S.; Migdall-Wilson, J.; Schlegel, J.; McGranahan, A.; Gao, D.; Liang, X.; DeRyckere, D. Inhibition of MerTK Increases Chemosensitivity and Decreases Oncogenic Potential in T-Cell Acute Lymphoblastic Leukemia. *Blood Cancer Journal* **2013**, *3* (1), e101. (d) Linger, R. M.; Lee-Sherick, A. B.; Deryckere, D.; Cohen, R. A.; Jacobsen, K. M.; McGranahan, A.; Brandão, L.; Winges, A.; Sawczyn, K. K.; Liang, X.; Keating, A. K.; Tan, A. C.; Earp, H. S.; Graham, D. K. Mer Receptor Tyrosine Kinase Is a Therapeutic Target in Pre-B Cell Acute

Lymphoblastic Leukemia. *Blood* **2013**, *122*, 1599−1609. (e) Knubel, K. H.; Pernu, B. M.; Sufit, A.; Nelson, S.; Pierce, A. M.; Keating, A. K. MerTK Inhibition is a Novel Therapeutic Approach for Glioblastoma Multiforme. *Oncotarget* **2014**, *5* (5), 1338−1351.

(12) (a) Abu-Duhier, F. M.; Goodeve, A. C.; Wilson, G. A.; Gari, M. A.; Peake, I. R.; Rees, D. C.; Vandenberghe, E. A.; Winship, P. R.; Reilly, J. T. FLT3 Internal Tandem Duplication Mutations in Adult Acute Myeloid Leukaemia Define a High-Risk Group. *Br. J. Hamaetol.* **2000**, *111* (1), 190−195. (b) Kottaridis, P. D.; Gale, R. E.; Frew, M. E.; Harrison, G.; Langabeer, S. E.; Belton, A. A.; Walker, H.; Wheatley, K.; Bowen, D. T.; Burnett, A. K.; Goldstone, A. H.; Linch, D. C. The Presence of a FLT3 Internal Tandem Duplication in Patients with Acute Myeloid Leukemia (AML) Adds Important Prognostic Information to Cytogenetic Risk Group and Response to the First Cycle of Chemotherapy: Analysis of 854 Patients from the United Kingdom Medical Research Council AML 10 and 12 Trials. *Blood* **2001**, *98* (6), 1752−1759.

(13) (a) Stone, R. M.; DeAngelo, D. J.; Klimek, V.; Galinsky, I.; Estey, E.; Nimer, S. D.; Grandin, W.; Lebwohl, D.; Wang, Y.; Cohen, P.; Fox, E. A.; Neuberg, D.; Clark, J.; Gilliland, D. G.; Griffin, J. D. Patients with Acute Myeloid Leukemia and an Activating Mutation in FLT3 Respond to a Small-Molecule FLT3 Tyrosine Kinase Inhibitor, PKC412. *Blood* **2005**, *105* (1), 54−60. (b) DeAngelo, D. J.; Stone, R. M.; Heaney, M. L.; Nimer, S. D.; Paquette, R. L.; Klisovic, R. B.; Caligiuri, M. A.; Cooper, M. R.; Lecerf, J. M.; Karol, M. D.; Sheng, S.; Holford, N.; Curtin, P. T.; Druker, B. J.; Heinrich, M. C. Phase 1 Clinical Results with Tandutinib (MLN518), a Novel FLT3 Antagonist, In Patients with Acute Myelogenous Leukemia or High-Risk Myelodysplastic Syndrome: Safety, Pharmacokinetics, And Pharmacodynamics. *Blood* **2006**, *108* (12), 3674−3681. (c) Knapper, S.; Burnett, A. K.; Littlewood, T.; Kell, W. J.; Agrawal, S.; Chopra, R.; Clark, R.; Levis, M. J.; Small, D. A Phase 2 Trial of the FLT3 Inhibitor Lestaurtinib (CEP701) as First-Line Treatment for Older Patients with Acute Myeloid Leukemia Not Considered Fit for Intensive Chemotherapy. *Blood* **2006**, *108* (10), 3262−3270.

(14) Pratz, K. W.; Luger, S. M. Will FLT3 inhibitors fulfill their promise in acute meyloid leukemia? *Curr. Opin. Hematol.* **2014**, *21* (2), 72−78.

(15) (a) Liu, J.; Yang, C.; Simpson, C.; DeRyckere, D.; Van, D. A.; Miley, M. J.; Kireev, D.; Norris-Drouin, J.; Sather, S.; Hunter, D.; Korboukh, V. K.; Patel, H. S.; Janzen, W. P.; Machius, M.; Johnson, G. L.; Earp, H. S.; Graham, D. K.; Frye, S. V.; Wang, X. Discovery of Small Molecule Mer Kinase Inhibitors for the Treatment of Pediatric Acute Lymphoblastic Leukemia. *ACS Med. Chem. Lett.* **2012**, *3*, 129−134. (b) Liu, J.; Zhang, W.; Stashko, M. A.; DeRyckere, D.; Cummings, C. T.; Hunter, D.; Yang, C.; Jayakody, C. N.; Cheng, N.; Simpson, C.; Norris-Drouin, J.; Sather, S.; Kireev, D.; Janzen, W. P.; Earp, H. S.; Graham, D. K.; Frye, S. V.; Wang, X. UNC1062, a New and Potent Mer Inhibitor. *Eur. J. Med. Chem.* **2013**, *65*, 83−93. (c) Zhang, W.; Zhang, D.; Stashko, M. A.; DeRyckere, D.; Hunter, D.; Kireev, D.; Miley, M. J.; Cummings, C.; Lee, M.; Norris-Drouin, J.; Stewart, W. M.; Sather, S.; Zhou, Y.; Kirkpatrick, G.; Machius, M.; Janzen, W. P.; Earp, H. S.; Graham, D. K.; Frye, S. V.; Wang, X. Pseudo-Cyclization through Intramolecular Hydrogen Bond Enables Discovery of Pyridine Substituted Pyrimidines as New Mer Kinase Inhibitors. *J. Med. Chem.* **2013**, *56* (23), 9683−9692. (d) Zhang, W.; McIver, A. L.; Stashko, M. A.; Deryckere, D.; Branchford, B. R.; Hunter, D.; Kireev, D.; Miley, M. J.; Norris-Drouin, J.; Stewart, W. M.; Lee, M.; Sather, S.; Zhou, Y.; Di Paola, J. A.; Machius, M.; Janzen, W. P.; Earp, H. S.; Graham, D. K.; Frye, S. V.; Wang, X. Discovery of mer Specific Tyrosine Kinase Inhibitors for the Treatment and Prevention of Thrombosis. *J. Med. Chem.* **2013**, *56* (23), 9693−9700.

(16) (a) Huang, X.; Finerty, P., Jr.; Walker, J. R.; Butler-Cole, C.; Vedadi, M.; Schapira, M.; Parker, S. A.; Turk, B. E.; Thompson, D. A.; Dhe-Paganon, S. Structural Insights into the Inhibited States of the Mer Receptor Tyrosine Kinase. *J. Struct Biol.* **2009**, *165* (2), 88−96. (b) Greshock, J.; Bachman, K. E.; Degenhardt, Y. Y.; Jing, J.; Wen, Y. H.; Eastman, S.; McNeil, E.; Moy, C.; Wegrzyn, R.; Auger, K.; Hardwicke, M. A.; Wooster, R. Molecular Target Class Is Predictive of In vitro Response Profile. *Cancer Res.* **2010**, *70* (9), 3677−3686. (c) Howard, S.; Berdini, V.; Boulstridge, J. A.; Carr, M. G.; Cross, D. M.; Curry, J.; Devine, L. A.; Early, T. R.; Fazal, L.; Gill, A. L.; Heathcote, M.; Maman, S.; Matthews, J. E.; McMenamin, R. L.; Navarro, E. F.; O'Brien, M. A.; O'Reilly, M.; Rees, D. C.; Reule, M.; Tisi, D.; Williams, G.; Vinkovic, M.; Wyatt, P. G. Fragment-Based Discovery of the Pyrazol-4-yl urea (AT9283), a Multitargeted Kinase Inhibitor with Potent Aurora Kinase Activity. *J. Med. Chem.* **2009**, *52* (2), 379−388. (d) Schroeder, G. M.; An, Y.; Cai, Z. W.; Chen, X. T.; Clark, C.; Cornelius, L. A.; Dai, J.; Gullo-Brown, J.; Gupta, A.; Henley, B.; Hunt, J. T.; Jeyaseelan, R.; Kamath, A.; Kim, K.; Lippy, J.; Lombardo, L. J.; Manne, V.; Oppenheimer, S.; Sack, J. S.; Schmidt, R. J.; Shen, G.; Stefanski, K.; Tokarski, J. S.; Trainor, G. L.; Wautlet, B. S.; Wei, D.; Williams, D. K.; Zhang, Y.; Fargnoli, J.; Borzilleri, R. M. Discovery of *N*-(4-(2-amino-3-chloropyridin-4-yloxy)-3-fluorophenyl)-4-ethoxy-1-(4-fluorophenyl)-2-oxo-1,2-dihydropyridine-3-carboxamide (BMS-777607), a Selective and Orally Efficacious Inhibitor of the Met Kinase Superfamily. *J. Med. Chem.* **2009**, *52* (5), 1251−1254. (e) Kataoka, Y.; Mukohara, T.; Tomioka, H.; Funakoshi, Y.; Kiyota, N.; Fujiwara, Y.; Yashiro, M.; Hirakawa, K.; Hirai, M.; Minami, H. Foretinib (GSK1363089), a Multi-Kinase Inhibitor of MET and VEGFRs, Inhibits Growth of Gastric Cancer Cell Lines by Blocking Inter-Receptor Tyrosine Kinase Networks. *Invest. New Drugs* **2012**, *30* (4), 1352−1360. (f) Yan, S. B.; Peek, V. L.; Ajamie, R.; Buchanan, S. G.; Graff, J. R.; Heidler, S. A.; Hui, Y. H.; Huss, K. L.; Konicek, B. W.; Manro, J. R.; Shih, C.; Stewart, J. A.; Stewart, T. R.; Stout, S. L.; Uhlik, M. T.; Um, S. L.; Wang, Y.; Wu, W.; Yan, L.; Yang, W. J.; Zhong, B.; Walgren, R. A. LY2801653 is an Orally Bioavailable Multi-Kinase Inhibitor with Potent Activity against MET, MST1R, and Other Oncoproteins, And Displays Anti-Tumor Activities in Mouse Xenograft Models. *Invest. New Drugs* **2013**, *31* (4), 833−844. (g) Katz, J. D.; Jewell, J. P.; Guerin, D. J.; Lim, J.; Dinsmore, C. J.; Deshmukh, S. V.; Pan, B. S.; Marshall, C. G.; Lu, W.; Altman, M. D.; Dahlberg, W. K.; Davis, L.; Falcone, D.; Gabarda, A. E.; Hang, G.; Hatch, H.; Holmes, R.; Kunii, K.; Lumb, K. J.; Lutterbach, B.; Mathvink, R.; Nazef, N.; Patel, S. B.; Qu, X.; Reilly, J. F.; Rickert, K. W.; Rosenstein, C.; Soisson, S. M.; Spencer, K. B.; Szewczak, A. A.; Walker, D.; Wang, W.; Young, J.; Zeng, Q. Discovery of a 5H-Benzo[4,5]cyclohepta[1,2-b]pyridin-5-one (MK-2461) Inhibitor of c-Met Kinase for the Treatment of Cancer. *J. Med. Chem.* **2011**, *54* (12), 4092−4108.

(17) Frye, S. V. The Art of the Chemical Probe. *Nat. Chem. Biol.* **2010**, *6* (3), 159−161.

(18) Liu, J.; Wang, X. Microwave-Assisted, Divergent Solution-Phase Synthesis of 1,3,6-Trisubstituted Pyrazolo[3,4-d]pyrimidines. *ACS Comb. Sci.* **2011**, *13* (4), 414−420.

(19) Palmer, D. S.; McDonagh, J. L.; Mitchell, J. B.; van Mourik, T.; Fedorov, M. V. First-Principles Calculation of the Intrinsic Aqueous Solubility of Crystalline Druglike Molecules. *J. Chem. Theory Comput.* **2012**, *8* (9), 3322−3337.

(20) Veith, H.; Southall, N.; Huang, R.; James, T.; Fayne, D.; Artemenko, N.; Shen, M.; Inglese, J.; Austin, C. P.; Lloyd, D. G.; Auld, D. S. Comprehensive Characterization of Cytochrome P450 Isozyme Selectivity Across Chemical Libraries. *Nat. Biotechnol.* **2009**, *27* (11), 1050−1055.

(21) (a) Diana, G. D.; Rudewicz, P.; Pevear, D. C.; Nitz, T. J.; Aldous, S. C.; Aldous, D. J.; Robinson, D. T.; Draper, T.; Dutko, F. J. Picornavirus Inhibitors: Trifluoromethyl Substitution Provides a Global Protective Effect against Hepatic Metabolism. *J. Med. Chem.* **1995**, *38* (8), 1355−1371. (b) Meanwell, N. A. Synopsis of Some Recent Tactical Application of Bioisosteres in Drug Design. *J. Med. Chem.* **2011**, *54* (8), 2529−2591.

(22) Bach, R. D.; Dmitrenko, O. Strain Energy of Small Ring Hydrocarbons. Influence of C-H Bond Dissociation Energies. *J. Am. Chem. Soc.* **2004**, *126* (13), 4444−4452.

(23) Wenglowsky, S.; Moreno, D.; Rudolph, J.; Ran, Y.; Ahrendt, K. A.; Arrigo, A.; Colson, B.; Gloor, S. L.; Hastings, G. Pyrazolopyridine Inhibitors of B-Raf ^{V600E}. Part 3: An Increase in Aqueous Solubility via

the Disruption of Crystal Packing. *Bioorg. Med. Chem. Lett.* **2012**, *22* (2), 912−915.
(24) Schuürer, S. C.; Muskal, S. M. Kinome-Wide Activity Modeling from Diverse Public High-Quality Data Sets. *J. Chem. Inf. Model.* **2013**, *53* (1), 27−38.
(25) Kitagawa, D.; Yokota, K.; Gouda, M.; Narumi, Y.; Ohmoto, H.; Nishiwaki, E.; Akita, K.; Kirii, Y. Activity-Based Kinase Profiling of Approved Tyrosine Kinase Inhibitors. *Genes Cells* **2013**, *18* (2), 110−122.
(26) Anastassiadis, T.; Deacon, S. W.; Devarajan, K.; Ma, H.; Peterson, J. R. Comprehensive assay of kinase catalytic activity reveals features of kinase inhibitor selectivity. *Nat. Biotechnol.* **2011**, *29* (11), 1039−1045.
(27) (a) Morrison, J. F. Kinetics of the Reversible Inhibition of Enzyme-Catalysed Reactions by Tight-Binding Inhibitors. *Biochim. Biophys. Acta* **1969**, *185* (2), 269−286. (b) Copeland, R. A. Evaluation of Enzyme Inhibitors in Drug Discovery. A guide for Medicinal Chemists and Pharmacologists. *Methods Biochem. Anal.* **2005**, *46*, 178−189.
(28) Patricelli, M. P.; Nomanbhoy, T. K.; Wu, J.; Brown, H.; Zhou, D.; Zhang, J.; Jagannathan, S.; Aban, A.; Okerberg, E.; Herring, C.; Nordin, B.; Weissig, H.; Yang, Q.; Lee, J. D.; Gray, N. S.; Kozarich, J. W. In Situ Kinase Profiling Reveals Functionally Relevant Properties of Native Kinases. *Chem. Biol.* **2011**, *18* (6), 699−710.
(29) Walters, D. K.; Stoffregen, E. P.; Heinrich, M. C.; Deininger, M. W.; Druker, B. J. RNAi-Induced down-Regulation of FLT3 Expression in AML Cell Lines Increases Sensitivity to MLN518. *Blood* **2005**, *105* (7), 2952−2954.